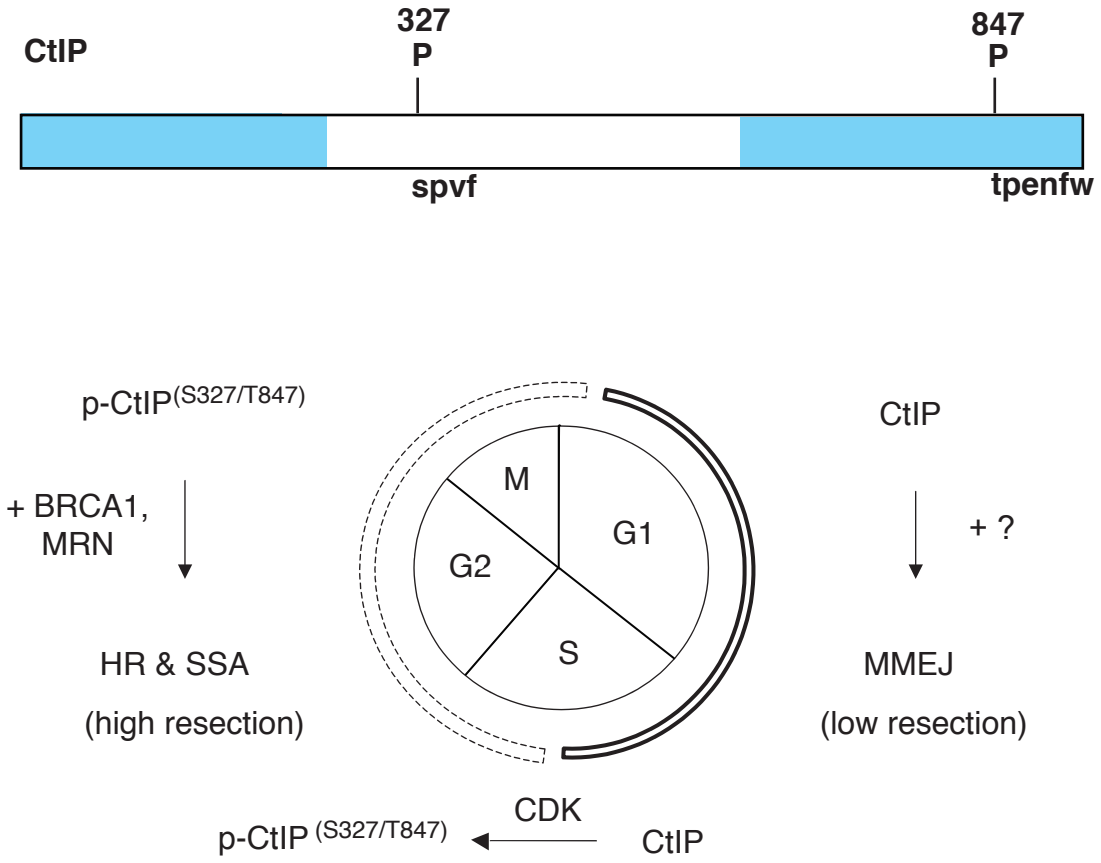

Suppl. Fig S1. Model depicting the role of CtIP in the regulation of DSB repair in vertebrates. Upper panel. Diagram of CtIP protein showing two potential CDK phosphorylation sites and surrounding amino acid sequence. Blue shading represents coiled-coil domains.

Lower panel. Phosphorylation of CtIP functions as a cell-cycle-dependent switch between DNA end-joining and HR pathways in the repair of DSB. In G1 phase expression of CtIP is low and serine residue 327 and threonine 847 are unphosphorylated. This form of the protein contributes to the repair of DSB through microhomology mediated end joining (MMEJ) by facilitating low level resection of broken DNA ends. During S phase CtIP becomes phosphorylated on S327 and T874 most likely through the action of CDKs. Phosphorylation of S327 promotes the interaction between CtIP and BRCA1 and leads to increased DNA end resection and upregulation of DSB repair by homologous recombination (including single strand annealing-SSA). The mechanism through which phosphorylation of T847 activates DNA resection and HR is unknown. Hence phosphorylation of CtIP and the recruitment of BRCA1 switches repair of DSB from error-prone MMEJ to error-free HR as cells progress through S phase, increasing the fidelity of repair and promoting genetic stability in the face of DNA damage.

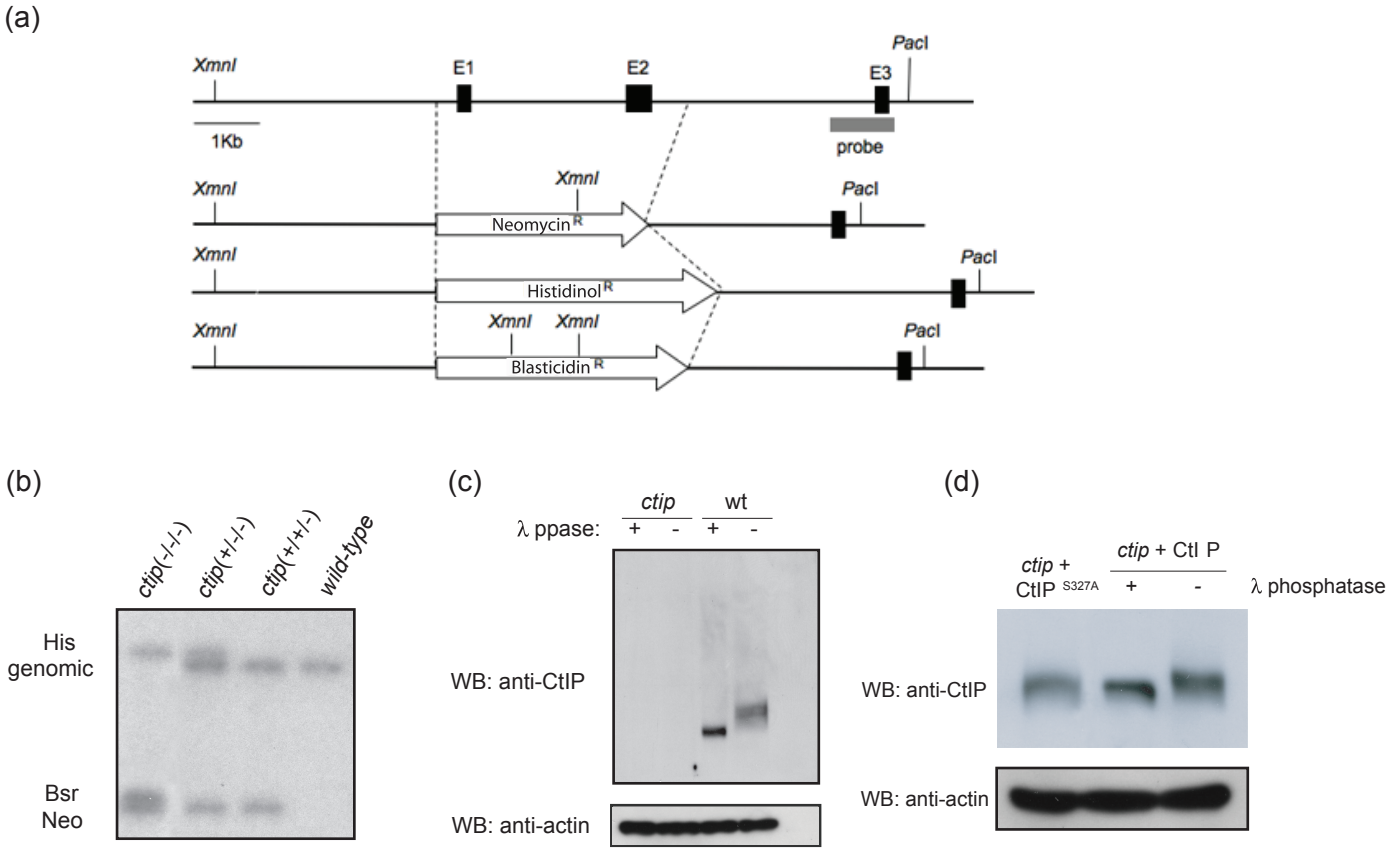

Suppl. Fig. S2. Generation of a *ctip* knockout in the Dt40 cell line

(a) Restriction map of the 5' region of the *CtIP* genomic locus in chromosome 2 of the Dt40 genome. Diagnostic restriction sites, exons (E1-3) and targeted alleles are shown. (b) Southern-blot analysis confirming the disruption of *CtIP* in Dt40 cells. Double digest with *Xmn*I and *Pac*I give bands of 9.5kb, 4.4kb, 9.9kb and 5.0Kb for the wt allele, for the neomycin-disrupted allele, for the histidinol-disrupted allele and for the blasticidin-disrupted allele respectively. (c) Western-blot showing the absence of CtIP or its phosphorylated forms in the knockout cell line (upper panel). Whole cell extracts from Dt40 wt or *ctip* cells were treated or not with λ phosphatase for 2hs before loading. The same samples were inmunoblotted against actin as protein loading control -lower pannel-. (d) CtIP expression in *ctip* complemented cell lines. Western blots performed with anti-*Hs*CtIP antibody (upper panel) or anti-actin antibody as protein loading control (lower panel) are shown. *ctip* mutant cells were stably trasfected with pcDNA3.1-*hs*CtIP or pcDNA3.1-*hs*CtIP(S327A) vectors. Complemented clones were selected by zeocin treatment and assessed for CtIP expression levels through inmunobloting of whole cell extracts. Only the clones selected for the experiments presented are shown.

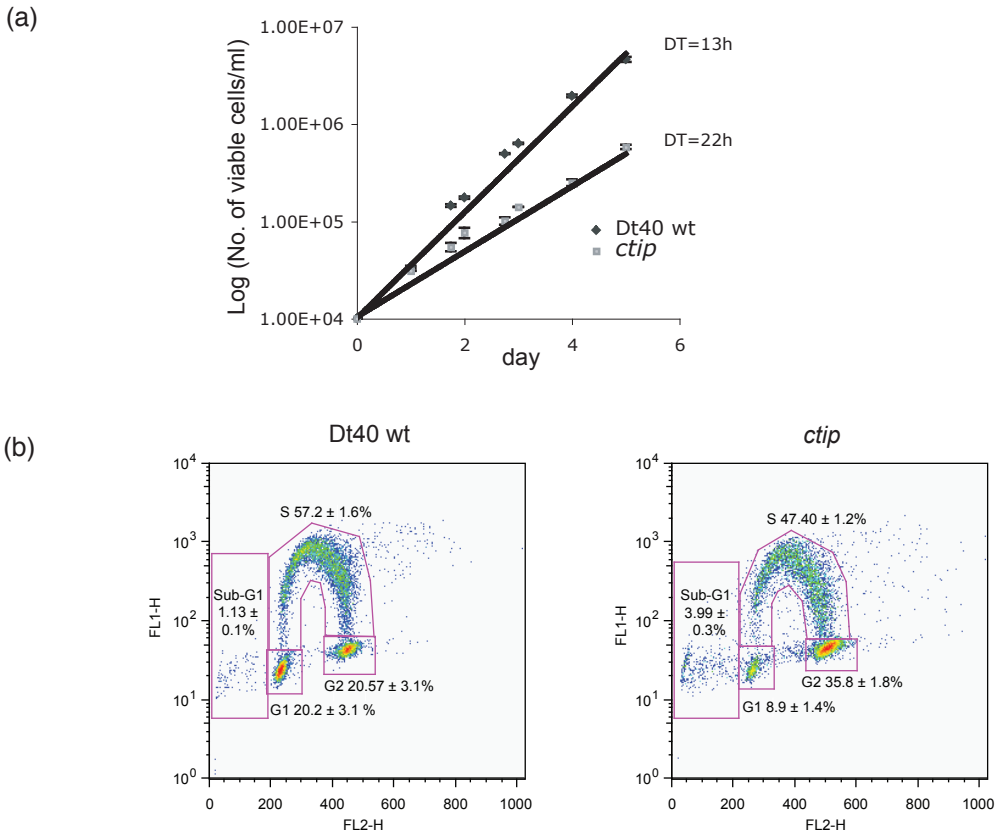

Suppl. Fig S3. Proliferation defects of a *ctip* mutant cell line

(a) Proliferative characteristics of Dt40 wt and ctip mutant cell lines. Growth curves correspond to the indicated cell cultures. Number of viable cells is expressed in logaritmic scale. The doubling times for each cell line were calculated after logarithmic transformation.Data shown are the average of three independent experiments. (b) Cell cycle distribution of the indicated Dt40 wt or *ctip* mutant cells as measured by BrdU and propidium iodide incorporation in flow cytometry analysis. Cells were pulse-labelled withBrdU for 15 minutes, fixed and subsequently stained with anti-BrdU primary antibody followed by a FITC-conjugated secondary antibody. BrdU incorporation is measured in the vertical axis -log scale- and PI incorporation in the horizontal axis -linear scale-. Cell cycle phases are indicated in each gate. The mean percentage of cells in each category and associated standard deviation for three independent experiments is shown.

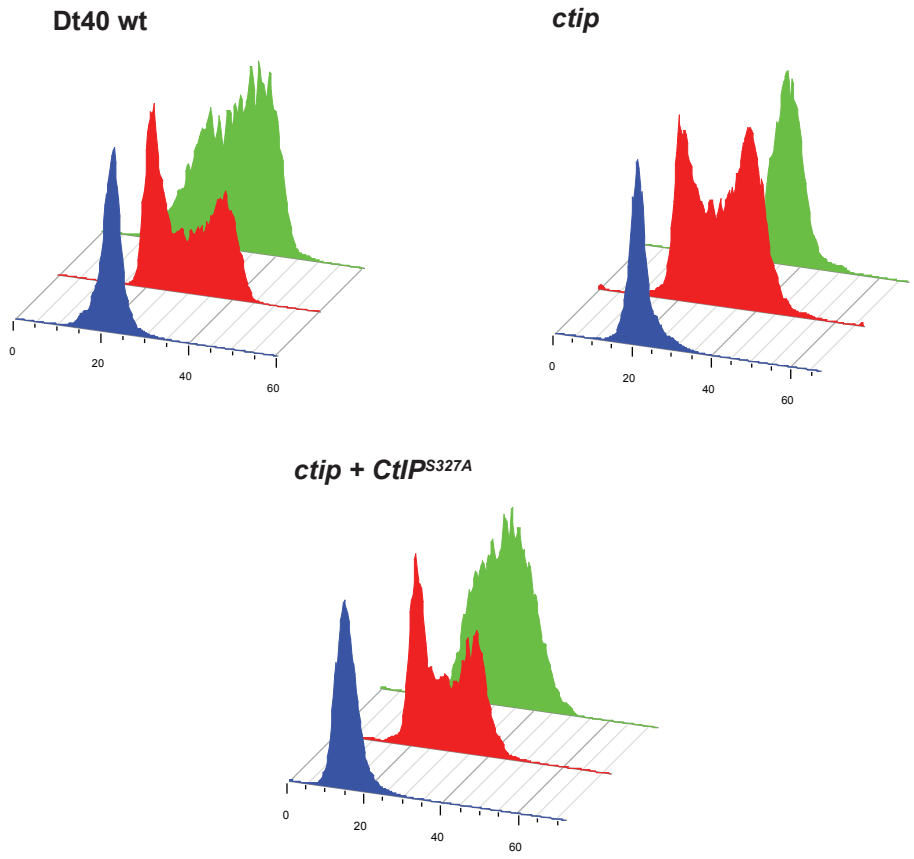

Suppl. Fig. S4. Centrifugal elutriation of DT40 cells
Representative cell cycle profiles of G1 (blue), S/G2 (green) and asynchronous (red) fractions for the indicated cell lines. Cells were separated by elutriation, resuspended in cold PBS and a fraction of them were stained with the cell-permeable dye Draq5 for 10 minutes, after which cell cycle profiles were obtained by FACS analysis.

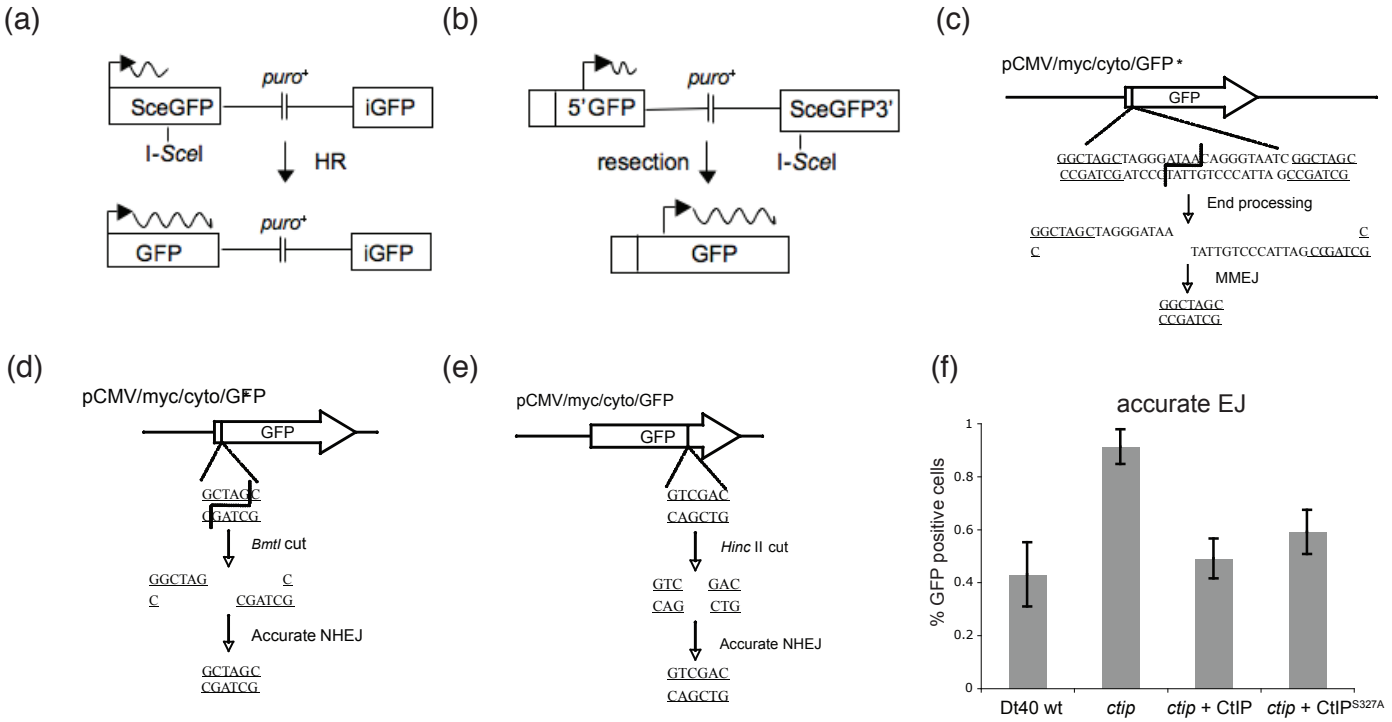

Suppl. Fig. S5. GFP-based DSB repair assays in Dt40 cells

(a) Schematic of HR assay. Transient expression of I-*Sce*I generates a specific double-strand break in the stably integrated SceGFP gene, which has two in-frame stop codons leading to an inactive protein. Functional GFP is only produced when the I-*Sce*I-induced break is repaired by HR using the internal GFP fragment (iGFP) as template.

(b) Schematic of the SSA assay. Transient expression of I-*Sce*I generates a specific double-strand break in the stably integrated 3'SceGFP gene, containing the 3' of the GFP gene only. Functional GFP is only produced when the I-*Sce*I induced break is repaired by SSA between 3'SceGFP and an upstream fragment containing the 5' region of the GFP gene (5'GFP) plus a region of homology with 3'SceGFP.

(c) Schematic of the MMEJ assay. The vector pCMV/myc/cyto/GFP* was modified by inserting a 28bp oligonucleotide containing an I-*Sce*I siteflanked by 7bp microhomology (underlined) inside the GFP sequence. This insertion introduces two stop codons and a frameshift, preventing GFP translation. Functional GFP is only generated after I-*Sce*I cutting and subsequent repair by MMEJ.

(d) Schematic of accurate end joining assay. Indicated cell lines were transfected with pCMV/myc/cyto/GFP linearized with the restriction enzyme *Bmt*I, which generates ends with 5'- overhang and disrupts the GFP coding sequence unless it is accurately re-ligated.

(e) Schematic of a second accurate end-joining assay. Indicated cell lines were transfected with pCMV/myc/cyto/GFP linearized with the blunt cutting restriction enzyme *Hinc*II, which disrupts the GFP coding sequence unless it is accurately re-ligated.

(f) percentage of accurately ligated cells as measure by GFP expression after blunt-accurate end joining assay represented in (e). *ctip* cells expressing CtIP^{S327A} exhibit normal levels of accurate end-joining.

(a)

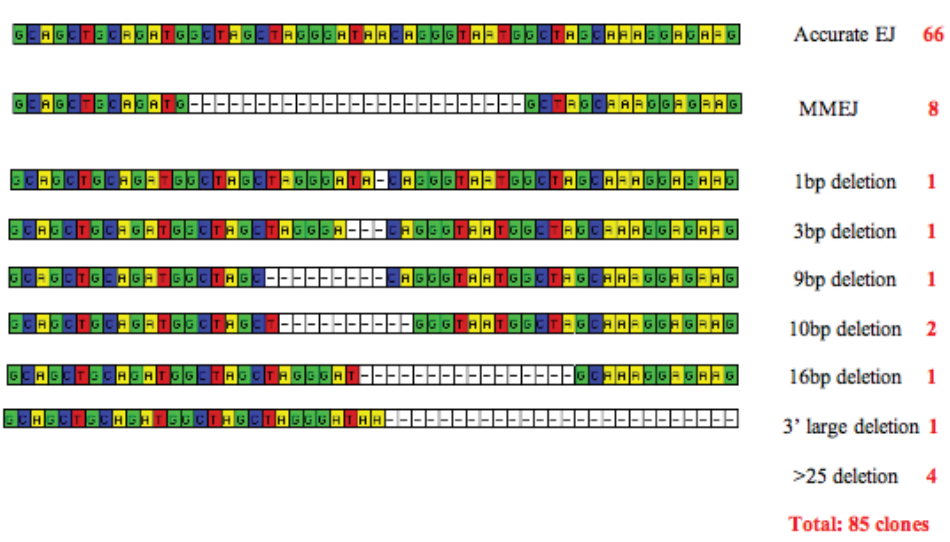

(b)

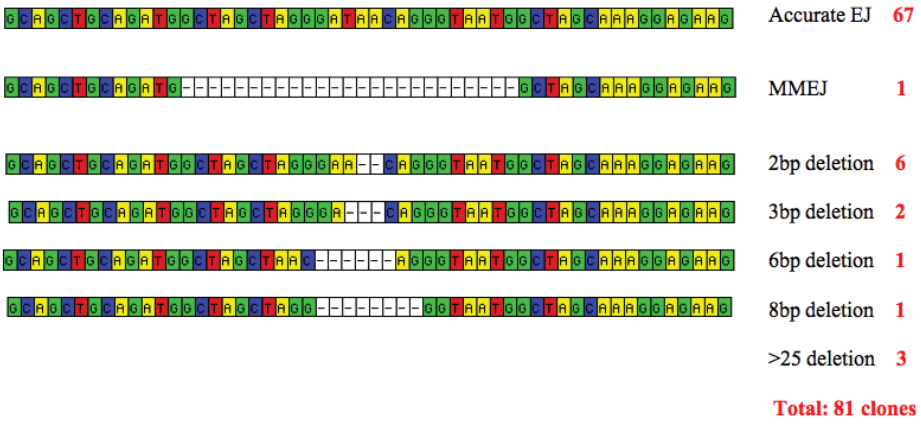

Suppl. Fig. S6. *ctip* mutant cells are defective in MMEJ

(a) Representative sequences of transfected plasmid after end-joining events. Dt40 wt cells were transfected with pCMV/cyto/GFP* I-*Sce*I digested to completion. After 24h plasmid DNA was extracted, treated with alkaline phosphatase to prevent ligation in bacteria and used in transformations. Screening of colonies was performed by ampicilin selection. 96 resistant colonies were selected and their plasmid DNA individually extracted and sequenced. (b) Representative sequences as in (a) but obtained in *ctip* mutant cells.

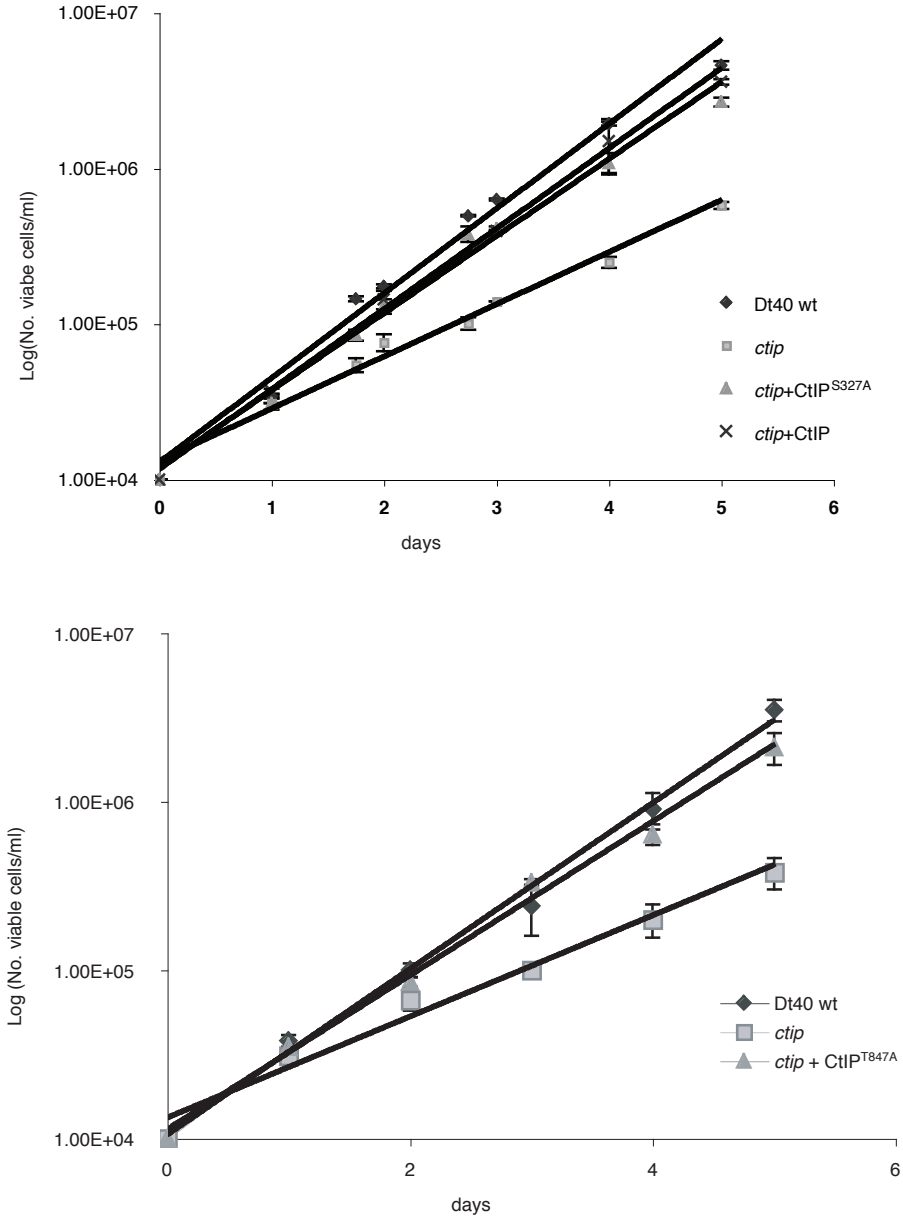

Suppl. Fig. S7. ctip mutant cells expressing CtIP^{T847A} or CtIP^{S327A} show no proliferation defects. Proliferative characteristics of ctip mutant cell lines complemented with *Hs*CtIP, HsCtIP^{S327A} (upper panel) and *Hs*CtIP^{T847A} (lower panel). Dt40 wild type and *ctip* mutant cell lines are shown for reference. Growth curves corresponding to the indicated cell cultures. Number of viable cells is expressed in logarithmic scale. Data shown are the average of three independent experiments.

(a)

(b)

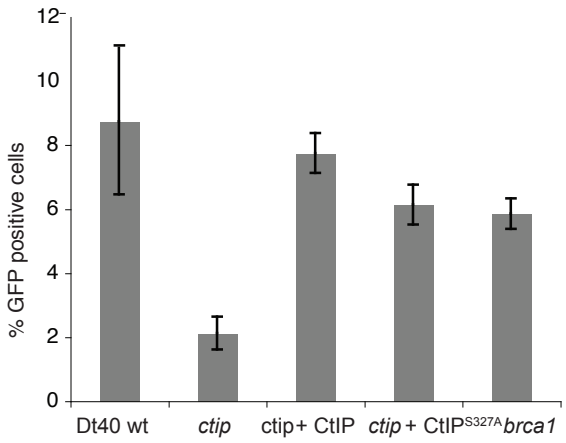

Suppl. Fig. S8. Brca1 is not required for MMEJ

(a) CtIP phosphorylation in S327 abrogates CtIP-BRCA1 interaction. Western blot anti CtIP after co-inmunoprecipitation of *Hs*CtIP or *Hs*CtIP^{S327A} with anti chicken BRCA1 or anti human CtIP antibodies from complemented ctip mutant cell extracts.

(b) MMEJ assay in Dt40 cells showing the relative percentage of GFP expressing cells. The indicated cell lines were transiently transfected with pCMV/myc/cyto/GFP (transfection efficiency control) or pCMV/myc/cyto/GFP* fully linearized with I-*Sce*I. The percentage of GFP positive cells was analysed 24h post-transfection by flow cytometry. Data shown are the mean of three independent experiments.

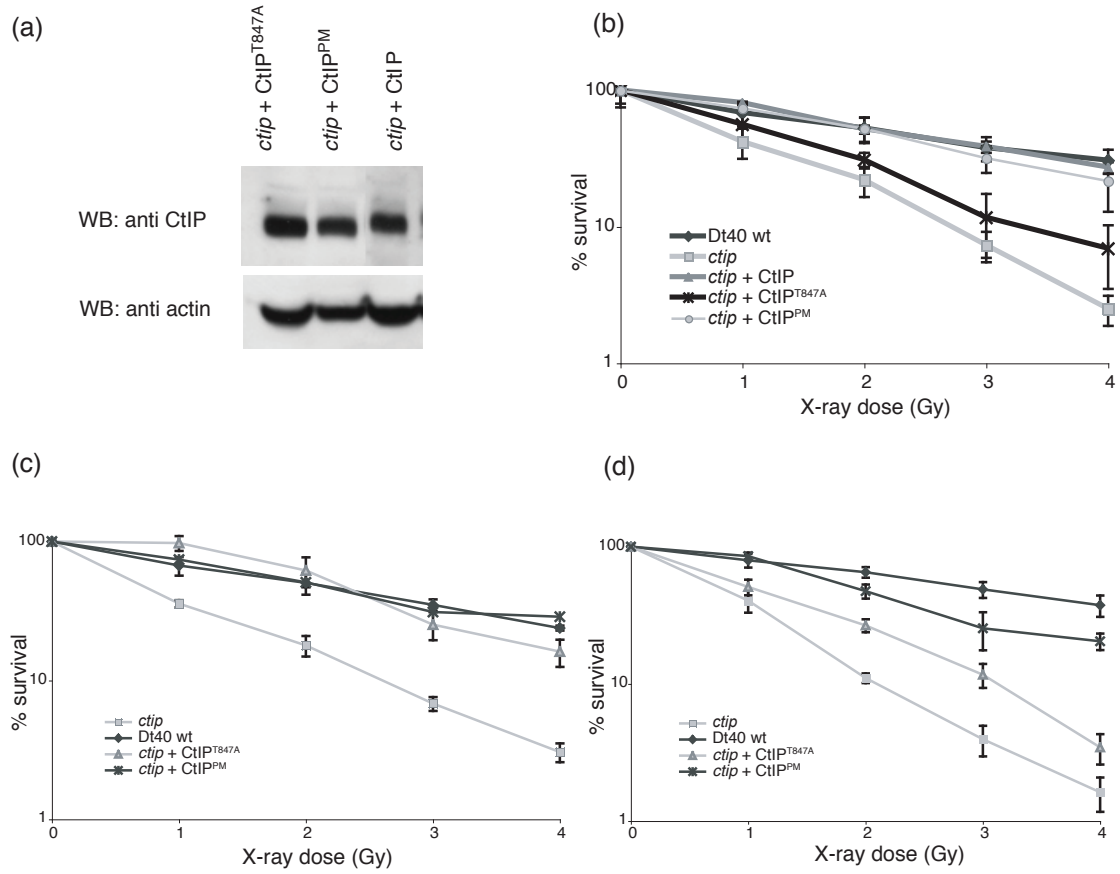

Suppl. Fig. S9. Phosphorylation of T847 on CtIP is required for tolerance to DNA damaging agents during S/G2.

(a) CtIP expression in complemented Dt40 *ctip* mutant cell lines. Western blots were peformed with anti CtIP antibody (upper panel) or anti actin antibody as protein loading control (lower panel). *ctip* mutant cells were transfected with pcDNA3.1-*Hs*CtIP, pcDNA3.1-*Hs*CtIP^{T847A} or pcDNA3.1-*Hs*CtIP^{T847E}(PM) vectors. Complemented clones were selected for zeocin resistance and whole cell extracts assessed for CtIP expression levels by immunoblotting.

(b) Methylcelulose colony survival assays were carried out with asynchronous cell populations after treating cells with the indicated doses of X-rays. Data are represent at least three independent experiments.

(c-d) Methylcellulose colony survival assay after X-ray treatment of the indicated cell line populations in either G1 (c) or S/G2 (d) stages of the cell cycle, selected using elutriation. Data represent three independent experiments.

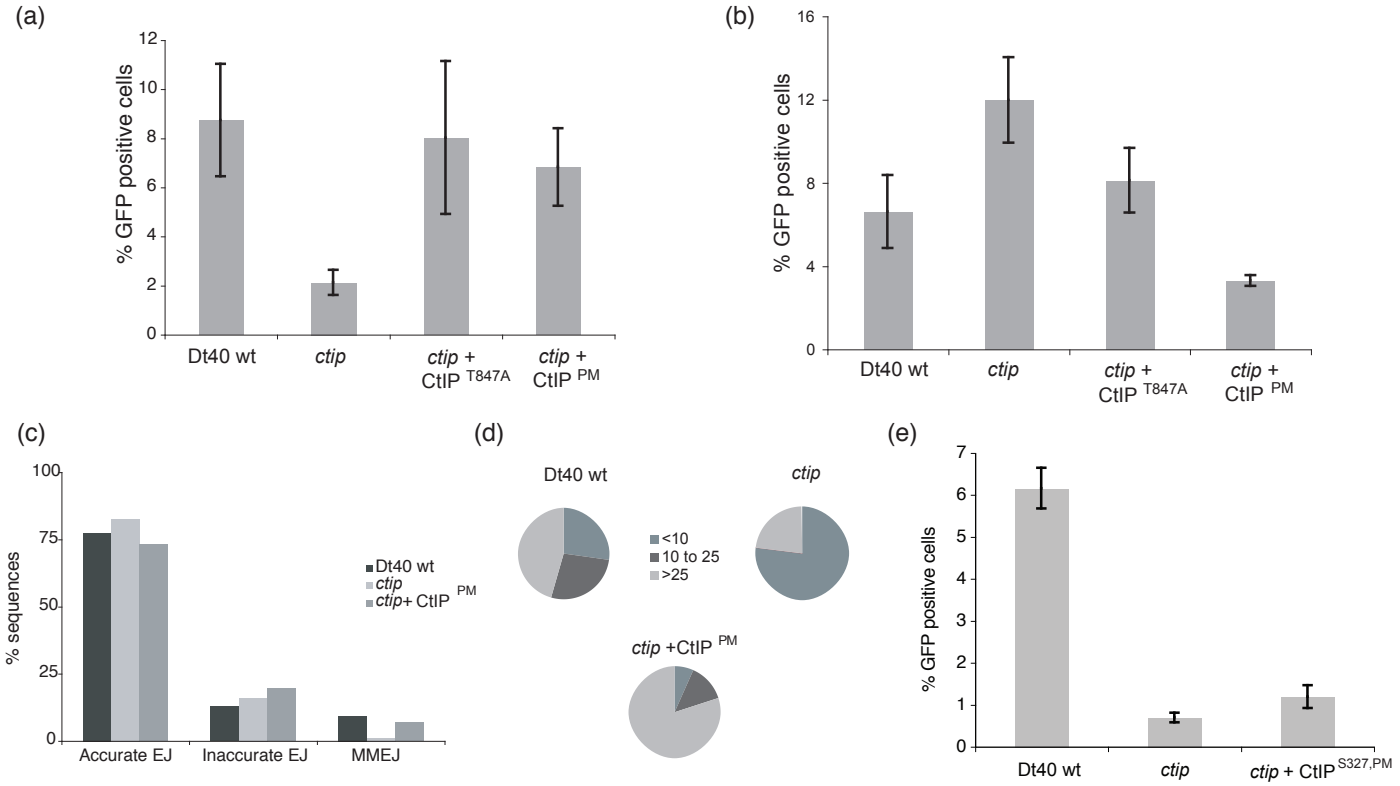

Suppl. Fig. S10. Phosphorylation of T847 on CtIP is not required for DNA end-joining.
(a) Phosphorylation of CtIP on residue T847 is not required for microhomology mediated end-joining. MMEJ assay was performed as described in Methods. Data represent of at least three independent experiments. (b) Phosphorylation of CtIP on T847 is not required for accurate end-joining. Accurate EJ assay was performed as described in Methods. Data represent at least three independent experiments. (c) Clasification of DNA repair events into accurate end-joining, inaccurate end-joining and micro-homology mediated end-joining for *ctip* mutant cells complemented with CtIP^{PM} as described in Methods. Dt40 wt and *ctip* mutatnt cell lines are presented for reference. Linearised plasmid was transfected into cells and repaired (circular) plasmid recovered and sequenced at the site of repair as described in Methods. (d) Classification of the innaccurate end-joining events obtained as in (c) in terms of the length of deletions surrounding the repaired break. Pie charts show the proportion of sequences in each category for each indicated cell line. (e) Homologous recombination assay (as described in Suppl. Fig.S5) showing that CtIP S327A mutation causes a defect in the repair of an I-*Sce*1 induced DNA break even when T847 is "activated' through the phosphomimic mata-tion CtIP^{PM}.

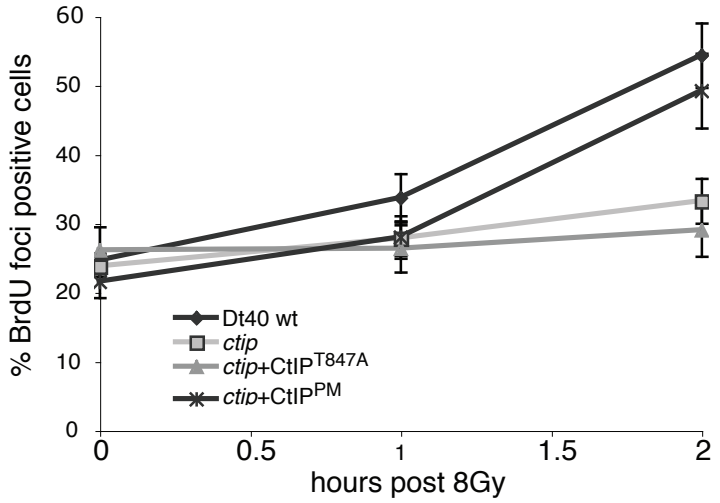

Suppl. Fig. S11. Phosphorylation of T847 on CtIP is required for the generation of ssDNA
BrdU-IF assay performed with the indicated cell lines as described in Methods and Fig 4.
Data presented are representative of three independent experiments. CtIP mutation T847A is defective in DNA resection but the phosphomimic mutation T847E (CtIP^{PM})is constitutively active for resection.

-